Available online at www.sciencedirect.com
ScienceDirect
Journal of Power Sources 161 (2006) 214–224
JOURNAL OF POWER SOURCES
www.elsevier.com/locate/jpowsour

On effective transport coefficients in PEM fuel cell electrodes: Anisotropy of the porous transport layers

J.G. Pharoah [a,b], K. Karan [a,c,*], W. Sun [a,c,1]

[a] *Queen's-RMC Fuel Cell Research Centre, 945 Princess Street, Kingston, Ont., Canada K7L 5L9*
[b] *Department of Mechanical and Materials Engineering, Queen's University at Kingston, Dupuis Hall, Division Street, Kingston, Ont., Canada K7L 3N6*
[c] *Department of Chemical Engineering, Queen's University at Kingston, Kingston, Ont., Canada K7L 3N6*

Received 17 January 2006; accepted 27 March 2006
Available online 23 June 2006

Abstract

This paper reviews the approach taken in the literature to model the effective transport coefficients – mass diffusivity, electrical conductivity, thermal conductivity and hydraulic permeability – of carbon-fibre based porous electrode of polymer electrolyte membrane fuel cells (PEMFCs). It is concluded that current PEMFC model do not account for the inherent anisotropic microstructure of the fibrous electrodes. Simulations using a 2-D PEMFC cathode model show that neglecting the anisotropic nature and associated transport coefficients of the porous electrodes significantly influences both the nature and the magnitude of the model predictions. This emphasizes the need to appropriately characterize the relevant anisotropic properties of the fibrous electrode.

Keywords: Gas diffusion layer; Fibrous porous media; Porous transport layer; Conductivity; Diffusivity

1. Introduction

The electrode of a polymer electrolyte membrane (PEM) fuel cell is a thin porous layer that connects the flow-field plate and the catalyst layer as shown in Fig. 1. This layer is commonly referred to in the literature as the gas diffusion layer (GDL). This term is restrictive and perhaps misleading in that it presupposes the primary function of the porous electrode to be gas diffusion when this is not the case. Accordingly, herein we use the term porous transport layer (PTL) to describe the porous electrode exclusive of the catalyst. The most commonly employed PTL for PEM fuel cells are carbon cloth and carbon paper. These materials are porous to allow for gas transport and electronically conducting to ensure electrons are transported to or from the catalyst sites. In addition, the pores of the PTL provide pathway for removal of liquid water generated in the cathode catalyst layer. Furthermore, the PTL helps to conduct heat to and from the catalyst layer and flow-field plates. Clearly, the PTL serves as a medium for transport of several different quantities.

In recent years there has been an increasing need to engineer the PTL such that some or all of the transport processes discussed above could be controlled. Mathematical modeling is an indispensible tool for exploring new architectures and designs of the PTL. However, appropriate characterization of the transport coefficients of a PTL is essential for meaningful predictions from such models. Over the past 20 years, numerous publications have been dedicated towards the modeling of polymer electrolyte membrane (PEM) fuel cells. In a recent comprehensive review of over 100 papers on mathematical modeling of PEM and direct methanol fuel cells [1], we found that in a majority of previous work, the transport of chemical species and electrons in the PTL were treated simplistically. For instance, most of the models for effective diffusive transport of chemical species and effective electronic conductivities in the PTL were based on correlations originally derived for granular porous me-

* Corresponding author at: Department of Chemical Engineering, Queen's University at Kingston, Kingston, Ont., Canada K7L 3N6. Tel.: +1 613 5333095; fax: +1 613 5336637.
[1] Present Address: Axion Power Inc., 100 Caster Ave., Woodbridge, Ont., Canada L4L 5Y9.
E-mail addresses: pharoah@me.queensu.ca (J.G. Pharoah), karan@chee.queensu.ca (K. Karan).

0378-7753/$ – see front matter © 2006 Elsevier B.V. All rights reserved.
doi:10.1016/j.jpowsour.2006.03.093

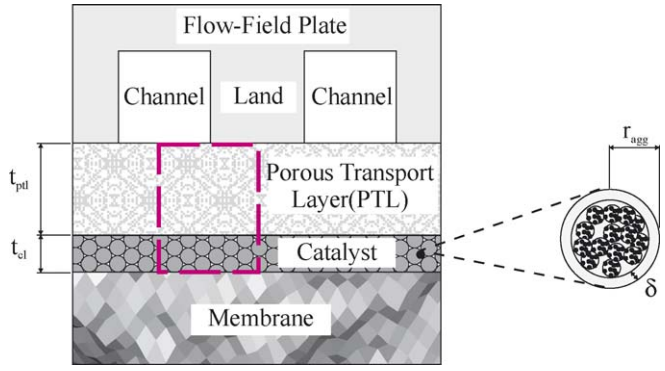

Fig. 1. Section of a PEMFC cathode (dotted line represents the solution domain for 2-D model).

dia. Unfortunately, the PTL microstructure does not resemble such a structure. A scanning electron micrograph of the carbon paper based PTL shown in Fig. 2 reinforces this point. The microstructure of the PTL can be described as randomly laid out cylindrical fibers 7–10 μm in diameter and several millimeters long. Usually hydrophobic material such as PTFE is added to the PTL, apparently to avoid liquid water flooding in the electrode [2]. It is clear that even without the added complexity of liquid water transport, the fibrous nature of PTL introduces anisotropy with respect to electron and gas transport. Thus, the commonly employed effective transport coefficients originally derived for granular porous media may not be appropriate for detailed PEMFC modeling.

A description of electron and chemical species transport that is representative of the physics of the process is essential because the local electrochemical reaction rates in the catalyst layers are a function of local species concentration and the local overpotential (related to electronic and ionic potentials), which are strongly influenced by transport through the PTL. In addition, it is known that convective transport does occur in the PTL [3], and so far, this directional dependance of the permeability has not been adequately addressed.

The objective of this paper is to review the approach taken to define the PTL effective transport coefficients. Further, using a 2-Dimensional model for PEMFC cathode we show that the choice of correlations has a significant impact on the prediction of local species fluxes, species composition and current densities. It is important to emphasize that most of the PEMFC models even with an incorrect transport coefficient can adequately fit selective experimental data (usually a polarization curve). However, such models may not be predictive and likely not provide insight into the influence of component design and properties on fuel cell performance.

2. Generalized potential driven transport

The four key transport processes occurring in the PTL are chemical species diffusion, electron conduction, thermal conduction and mass convection. Each of these processes are driven by the relevant specific potential. The flux associated with each of these processes depend on the gradient of the relevant potential and effective transport coefficient.

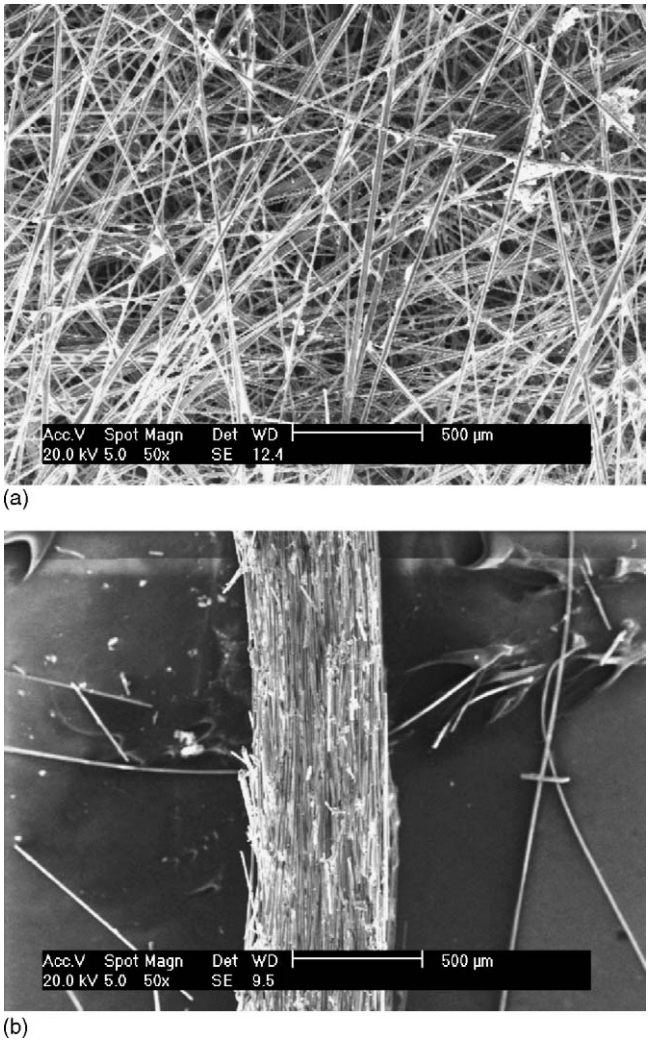

Fig. 2. Typical carbon fibre paper used as porous transport layer in PEM fuel cells. (a) Surface view (b) Edge view.

$$\text{Flux} = \Gamma^{\text{eff}} \nabla \phi \tag{1}$$

Table 1 summarizes the relevant potential and effective transport coefficients for the four processes occurring in the PTL. It is useful to point that the transport coefficient in itself depends on the inherent property of the transport medium and/or the transported species. However, these transport coefficients are modified to account for the effects of the microstructure of the transport media, which in the present context is the PTL.

Table 1
Key transport processes in PTL, associated driving potential and transport coefficient

Flux	Transport coefficient	Potential
n_i (mol m^{-2} s^{-1})	D_{im} (m^2 s^{-1})	C_i (mol m^{-3})
q (W m^{-2})	k (W m^{-1}K^{-1})	T (K)
i_{e} (A m^{-2})	σ_{e} (S m^{-1})	ϕ_{e} (V)
i_{p} (A m^{-2})	σ_{p} (S m^{-1})	ϕ_{P} (V)
v (m s^{-1})	k/μ (m^2 Pa^{-1} s^{-1})	P (Pa)

3. Effective chemical species diffusivity models

One of the main functions of the PTL is to allow species transport to and from the catalyst surface. Diffusion of chemical species is one of the key modes of transport of reactants from the flow-channels to the catalyst layer. For diffusion through porous material, the binary diffusion coefficient, D_{ij}, is modified to account for the effects of the microstructure of the porous media:

$$D_{ij}^{\text{eff}} = f(\varepsilon) \cdot D_{ij} \tag{2}$$

It must be noted that all microstructural effects are lumped in a function $f(\varepsilon)$ of a single parameter—porosity (ε). Various theories are available to determine the function $f(\varepsilon)$.

The Bruggeman relation is an analytic expression which belongs to the class of solutions referred to as Effective Medium Approximations. The chemical species diffusivity in the PTL is most commonly described by the Bruggeman's relation, wherein the characteristic function describing the porous microstructure is given by:

$$f(\varepsilon) = \varepsilon^{1.5} \tag{3}$$

Interestingly, this correlation was originally derived for effective dispersion medium permittivity of beds of spherical particles of differing sizes [4] and was later verified experimentally by measuring the conductivity of an electrolyte surrounding spherical glass beads. The relation fits experimental data for diffusivity in granular packed beds [5]. However, it appears that when this correlation was first adopted to describe mass diffusivity in fibrous PTL, the validity of the correlation applied to fibrous porous structures was not considered.

3.1. Diffusivity of gases in fibrous porous media

Except for a paper by Nam and Kaviany [6], none of the PEMFC models have considered the anisotropy of fibrous PTLs with respect to species diffusivity. It is interesting to note that a considerable amount of work, both theoretical and experimental, has been undertaken to understand and describe the phenomena of gas diffusivity in fibrous porous media. Tomadakis and Sotirchos [7,8] applied Monte Carlo simulation to estimate the effective diffusivity of chemical species in a packing of overlapping fibres randomly distributed in a plane. Nam and Kaviany [6] reported the correlation given by Eq. (4), originally reported by Tomadakis and Sotirchos [8], where $\alpha = 0.521$ for the in-plane direction, $\alpha = 0.785$ for the through-plane direction, and $\varepsilon_p = 0.11$.

$$f(\varepsilon) = \varepsilon \left[\frac{\varepsilon - \varepsilon_p}{1 - \varepsilon_p}\right]^{\alpha} \tag{4}$$

Fig. 3 compares the Bruggeman relation to the anisotropic percolation type correlation of Tomadakis and Sotirchos. It is to note, that with this model, the through-plane value is always lower than the in-plane value, and that the differences decrease with increasing porosity. At a porosity of 0.8, the in-plane value is only 91% of the value suggested by the Bruggeman relation, while at a porosity of 0.4, the in-plane value is only 65% of the Bruggeman relation. This indicates that when diffusion

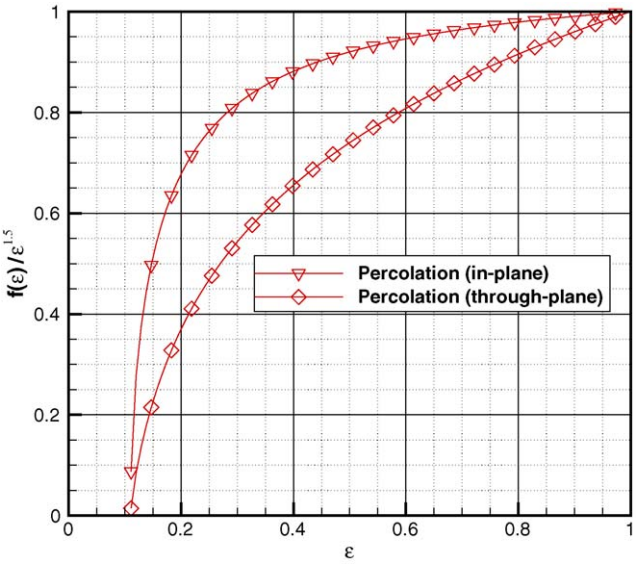

Fig. 3. Comparison of effective diffusivity from percolation theory with the Bruggeman correlation.

is an important mechanism the Bruggeman relation will overpredict the concentration of Oxygen in the catalyst layer and hence the current density. The extent of this effect is analyzed in Section 8.

4. Thermal conductivity

Contrary to some of the modeling results [9], experimental data [10] indicate that significant temperature gradients exist across the PTL. One likely reason that the models are unable to capture experimentally observed temperature gradients is that inaccurate and unrealistically large values for thermal conductivity of the PTL is employed in the model. In our survey of over 100 fuel cell modelling papers, every non-isothermal model used the volume averaged thermal conductivity. A physical interpretation of this volume-averaging is that of a porous media that is perfectly sorted such that all the solid material is parallel to all the void space, as shown in Fig. 4. This means that some of the heat energy is forced either to pass through the solid phase, and some is forced through the void phase but no path involving a combination of solid and void is allowed.

$$k_{\text{eff,parallel}} = \varepsilon k_v + (1 - \varepsilon) k_s \tag{5}$$

Another possible way of sorting the material is to stack regions of solid and regions of void such that all of the heat energy is forced to pass through both solid and void. This ordering corresponds to a series resistance network, and results in a volume weighted harmonic average for the effective conductivity.

$$k_{\text{eff,series}} = \frac{k_s k_v}{\varepsilon k_s + (1 - \varepsilon) k_v} \tag{6}$$

These two expressions are plotted in Fig. 4 for the case of $k_s/k_v = 100$, along with the series and parallel resistance networks from which they are derived. The parallel resistance provides an upper limit for the effective conductivity, while the series resistance network provides a lower limit. Clearly, real

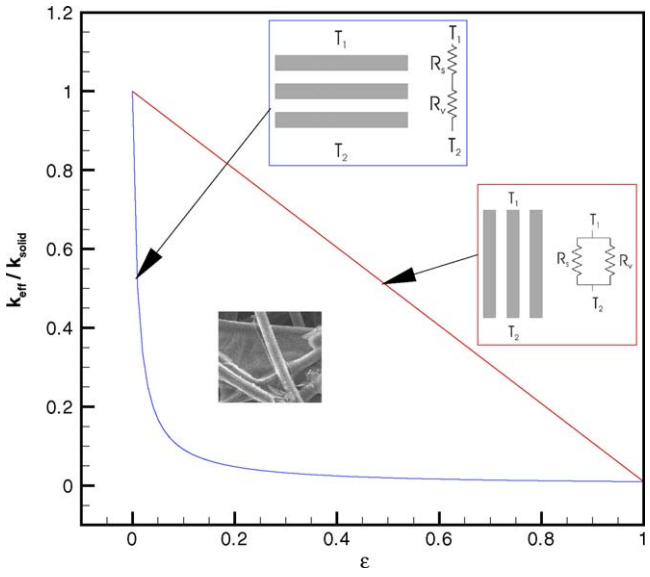

Fig. 4. Normalized thermal conductivity for series ordering and parallel ordering. $k_s/k_v = 100$.

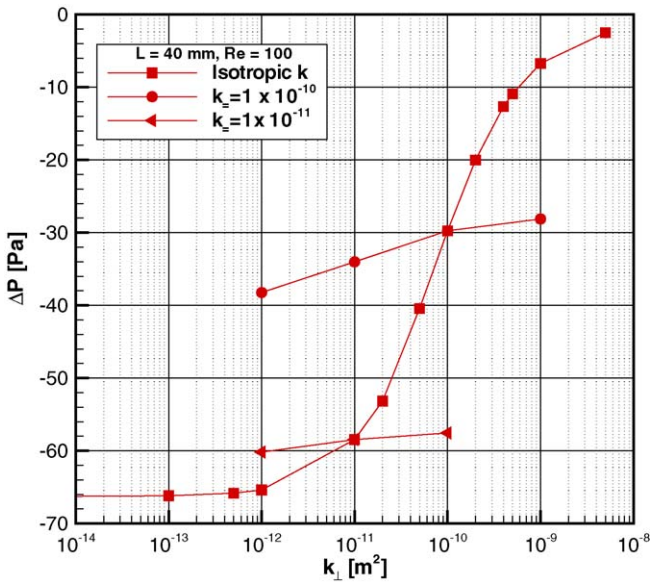

Fig. 5. The effect of anisotropic permeability on channel pressure drop. $Re = 100$, $L = 40$ mm.

porous media with random orderings of solid and void space must lie somewhere in between the two limits.

In a recently completed thesis [11] the anisotropic thermal conductivity of carbon fibre mattes was computed using a discretization of fibrous microstructures. The results indicate that the volume average, or parallel resistance model, significantly over-predicts the actual thermal conductivity which lies closer to the series approximation—especially in the in-plane direction. This means that predicted temperature gradients across the PTL will be significantly lower than in reality.

5. Electronic conductivity

Although several models, citing high electronic conductivity of the medium, ignore the electronic potential gradients in the PTL it has been shown [12–14] that the electron transport in the PTL can influence the distribution of current density or reaction rate in the catalyst layer. The effective electronic conductivity of PTL materials, to a first approximation, is analogous to the effective thermal conductivity in the limit of the void conductivity taken to zero. For series arrangement, the effective conductivity is zero because the inter-layer of void serves as a perfect insulator. The parallel arrangement yields the following expression for effective conductivity:

$$\sigma_{\text{eff,parallel}} = (1 - \varepsilon)\sigma_s \tag{7}$$

These approximations are seldom used and effective conductivity values instead are referenced from other papers or manufacturers web sites. It is only recently that the effect of anisotropic electronic conductivity has been investigated [14,15]. While there is very little experimental verification of anisotropic electronic conductivities, some evidence seems to suggest that the in-plane conductivity is about an order of magnitude higher than the through plane value [2]. It will be shown in section 8 that higher in-plane conductivities can drastically alter the location of current production by electrochemical reaction.

6. Hydraulic permeability

The permeability of PTL material is of most significance when serpentine flow fields are used because this induces an in-plane pressure gradient on the porous transport media. This pressure gradient results in the diversion of significant flow under the lands and causes a substantial decrease in the pressure drop required to drive the flow. This ‘feature’ has been demonstrated numerically [3], and has been exploited physically to detect flooding in the porous transport layer [16].

It can be expected that similar to other properties, the permeability of PTL materials is also likely to be anisotropic, though these values are not often reported. The relative importance of in-plane and through-plane permabilities was recently considered [3], and it was shown that the in-plane value is most significant. This is demonstrated in Fig. 5 which plots the pressure drop necessary to drive a fixed flow rate through a single serpentine channel mounted on PTLs of varying permeability. In the case of isotropic PTLs the pressure drop follows a sigmoidal type curve with a low pressure drop corresponding to high permeability and a much larger pressure drop in the limit of impermeable PTLs. In this case, an isotropic PTL is virtually impermeable when the permeability is of order 10^{-12} m^2. Interestingly, if the through-plane permeability is held constant while the in-plane permeability is increased, the driving pressure gradient decreases by over 40%. Unfortunately, virtually all measurements of PTL permeabilities correspond to the through-plane values. This can be very misleading, and accordingly, there is a significant need to characterize PTLs for in-plane permeability.

7. Porosity of the porous transport layer

As pointed out earlier, correlations describing effective transport coefficients account for porous media effects in terms of a single parameter—porosity. As such, porosity is an impor-

Fig. 6. Picture of a PTL showing localized compression under the land area [17] (dark striations correspond to PTL under the land area that have been subjected to compression).

tant model input parameter. Selecting a representative value of PTL porosity is complicated because in an operational fuel cell the PTL is subjected to spatially variant stress or compression, which in turn results in a spatially distributed porosity. For instance, the PTL under the land area is expected to be compressed to a greater extent than that under the channel, consequently PTL porosity is expected to be lower than that under the channel area. This effect is highlighted in Fig. 6, which shows a picture of a carbon-fibre based PTL that had been placed between two plates, each 12.7 cm × 12.7 cm – one which was flat and another plate with single serpentine channel – subjected to a stress of 1.2 MPa [17]. The dark striations correspond to the PTL that were under the land are were subjected to compression. The extent to which PTL porosity is compressed under various stress or mechanical load conditions has been reported by [18]. The extent of compression or more correctly strain was found to vary non-linearly with the applied stress. The porosity of uncompressed PTL can be over 80% [19,18] but as per data of Mishra and co-workers [18] it can reduce to 55–65% when subjected to local stress of 0.5–1 MPa. In contrast, much of the original PEMFC modeling work have employed a porosity value of 40%. In the following section, we examine the extent to which the PTL porosity influences performance of a PEMFC via simulations.

8. Effect of transport coefficients on the predictions of fuel cell performance

So far, we have discussed the applicability of various transport coefficients and the need for anisotropic transport coefficients on physical grounds. We will now demonstrate the impact of transport coefficients and their directional dependance on fuel cell performance using a simplified two-dimensional (2-D) PEMFC cathode model applied in the cross-channel plane.

8.1. 2D PEMFC cathode model

The details of the 2-D model formulation are given in [13,15]. The model accounts for the following key physico-electrochemical processes: multi-component diffusion of chemical species in the PTL and catalyst layer, oxygen dissolution and diffusion within idealized catalyst agglomerates, electron conduction in the PTL and catalyst layer, proton transport in the catalyst layer and electrochemical reaction governed by Butler–Volmer type kinetics.

The problem domain, which assumes symmetry at the channel centreline and the land centreline, is shown in Fig. 1. It is useful to note that this symmetry is not strictly valid for the case of convective transport under the lands, a situation not investigated in our 2-D model. The coupled transport-reaction equations are solved.

8.1.1. Species transport

The transport of chemical species in the PTL and the catalyst layer is modeled as multi-component diffusion in the porous media by the Maxwell–Stefan equation:

$$\nabla \cdot n_i = \nabla \cdot \left[-\rho w_i \sum_{i=1}^{i=n} D_{ij}^{\text{eff}} \frac{M}{M_j} \left(\nabla w_j + w_j \frac{\nabla M}{M} \right) \right] \tag{8}$$

where, n_i is mass flux (kg m^{-2} s^{-1}), ρ gas mixture density, and w_i is mass fraction of species i. The average molecular weight of gas mixture (M) is:

$$M = \sum x_i M_i \tag{9}$$

and the gas mixture density is is calculated by:

$$\rho = M \frac{P_{\text{tot}}}{RT_{\text{o}}} \tag{10}$$

In the catalyst layer, the gradient of oxygen molar flux (N_{O_2}) is equal to the rate of reaction:

$$\nabla \cdot N_{\text{O}_2} = -R_{\text{O}_2} \tag{11}$$

The rate of reaction, R_{O_2}, within the catalyst layer is described by the following equation:

$$R_{\text{O}_2} = C_{\text{O}_{2,\text{s}}} \left[\frac{1}{E_{\text{r}} k_{\text{c}} (1 - \varepsilon^{\text{cat}})} + \frac{(r_{\text{agg}} + \delta)\delta}{a_{\text{agg}} r_{\text{agg}} D} \right]^{-1} \tag{12}$$

The above Eq. (12) describes the rate of oxygen consumption in terms of the oxygen concentration at the agglomerate surface ($C_{\text{O}_{2,\text{s}}}$), an reaction effectiveness factor, E_{r}, to account for the diffusion-reaction process within the agglomerate, and an electrochemical rate constant, k_{c}. The reaction effectiveness factor for spherical agglomerate is calculated by:

$$E_{\text{r}} = \frac{1}{\phi_{\text{L}}} \left(\frac{1}{\tanh(3\phi_{\text{L}})} - \frac{1}{3\phi_{\text{L}}} \right) \tag{13}$$

where

$$\phi_{\text{L}} = \frac{r_{\text{agg}}}{3} \sqrt{\frac{k_{\text{c}}}{D_{\text{eff}}}} \tag{14}$$

$$D_{\text{eff}} = D\varepsilon^{1.5} \tag{15}$$

The electrochemical reaction rate, k_c, is essentially Butler–Volmer equation accounting for catalyst microstructure effects:

$$k_c = \left(\frac{\varepsilon_l m_{Pt} S_{ac}}{4Ft_{cl}(1-\varepsilon_{cat})}\right)\left[\frac{i_{0_{ref}}}{C_{O_{2,ref}}}\right] \times \left[\exp(\alpha_c f\eta) - \exp((1-\alpha_c) f\eta)\right] \quad (16)$$

where, $f = F/RT$ and $S_{ac} = 3/(r_{Pt}\rho_{Pt})$. All other parameters in the above Eq. 16 are reported in Table 3 and the variable η, the overpotential is an input variable. More details of the catalyst layer model are provided in [13].

8.1.2. Charge transport

The electron transport within the PTL is described by Ohm's law:

$$i_{e,\,PTL} = -k^{eff}_{s,\,PTL}\nabla\phi_s \quad (17)$$

also,

$$\nabla \cdot i_{e,\,PTL} = 0 \quad (18)$$

The effective conductivity of the PTL is specified as an input parameters for isotropic and anisotropic models.

The electron and proton transport within the catalyst layer are described by the following equations:

$$i_{e,\,cat} = -k^{eff}_{s,\,cat}\nabla\phi_s \quad (19)$$

$$i_{p,\,cat} = -k^{eff}_{l,\,cat}\nabla\phi_l \quad (20)$$

also,

$$\nabla(i_{e,\,cat} + i_{p,\,cat}) = 0 \quad (21)$$

and

$$\nabla \cdot i_{e,\,cat} = \nabla \cdot i \quad (22)$$

The effective conductivities of the proton and electron are calculated by Bruggeman relation because the catalysts are considered to be spherical agglomerates:

$$k^{eff}_{s,\,cat} = k_s[(1-\varepsilon_{cat})(1-\varepsilon_{agg})]^{1.5} \quad (23)$$

and

$$k^{eff}_{l,\,cat} = k_l[(1-\varepsilon_{cat})\varepsilon_{agg}]^{1.5} \quad (24)$$

The proton conductivity of the electrolyte membrane is represented as that of the Nafion and modeled in [13] according to the following equations based on work by Springer group [20]:

$$k_l = 100[0.005139\lambda - 0.00326]\exp\left[1268\left(\frac{1}{303} - \frac{1}{T}\right)\right] \quad (25)$$

and, the local water content, λ, in the electrolyte phase depends on the relative humidity (RH):

$$\lambda = 0.3 + 10.8RH - 16RH^2 + 14.1RH^3 \quad (26)$$

Table 2
Operating parameters considered in 2-D model

Inlet pressure (absolute) (atm)	1.5
Operating temperature (°C)	80
Inlet oxygen/nitrogen ratio	21/79
Inlet air relative humidity	50

Table 3
Input geometric and microstructural parameters

Parameters (units)	Value
PTL thickness (μm)	300
Porosity of PTL, ε_{PTL}	0.6
Pt loading, m_{Pt} (mg cm^{-2} Pt)	0.4
Pt particle diameter, r_{Pt} (nm)	2.5
Radius of agglomerate, r_{agg} (μm)	1
Effective specific agglomerate surface area, a_{agg} (m^2 m^{-3})	3.6×10^5
Catalyst layer thickness, t_{cl} (μm)	15
Porosity of catalyst layer, ε_{cat}	0.1
Electrolyte film covering each agglomerate, δ (nm)	80

8.1.3. Boundary conditions

For species transport, no flux boundary conditions was specified at the right, left and bottom sides of the domain in Fig. 1. At the top side of the domain, concentrations of oxygen, nitrogen and water vapor was specified at the interface between the PTL and the channel, whereas no flux boundary condition was implemented at the the interface between PTL and the land region. Similarly, for electron transport no flux boundary conditions was specified at the right, left and bottom sides of the domain. At the top side of domain, no flux boundary condition was implemented at the the interface between the PTL and the channel, whereas an electronic phase potential of zero was specified at the interface between the PTL and the land. For proton transport, again, no flux boundary conditions were specified at the right and left hand sides of the domain. The bottom side of the domain was set to proton phase potential equal to the specified overpotential whereas the interface between the PTL and the catalyst layer was set as no flux boundary.

The key model input parameters are provided in Tables 2–4. The details of how these parameters were obtained are provided

Table 4
Physical and electrochemical kinetic parameters

Parameters (units)	Value
Conductivity of PTL, k_s (S m^{-1})	100
O_2 Diffusivity in Nafion[a], D (m^{2}s^{-1})	8.45×10^{-10}
Binary diffusivities, D_{ij} (atm m^{2}s^{-1})	
$D_{O_2-H_2O}$	3.70×10^{-5}
$D_{O_2-N_2}$	2.79×10^{-5}
$D_{N_2-H_2O}$	3.87×10^{-5}
Cathodic transfer coefficient[a], α_c	
Low slope (≥0.8 V)	1
High slope (≤0.8 V)	0.61
Reference exchange current density[a], i_0 (A cm^{-2})	
Low slope (≥0.8 V)	3.85×10^{-8}
High slope (≤0.8 V)	1.5×10^{-6}
Reference O_2 concentration[b], $C_{O_{2,ref}}$(mol m^{-3})	0.85

[a] 80 °C.
[b] 80 °C and 1.5 atm.

in [13]. The governing equations with their associated boundary conditions were solved using the Multiphysics software FEMLAB (Comsol). The simulation results are presented in the following sub-sections. The effects of anisotropic mass diffusivity and electronic conductivity on the polarization curve and, more importantly, on the current density distribution in cross-channel direction are investigated.

8.2. Isotropic and anisotropic mass diffusivity

In this section we examine the influence of mass diffusivity magnitude by comparing three different effective diffusivity models at two different PTL porosity values. The three models are: (i) isotropic effective diffusivity calculated by Bruggeman relation, (ii) isotropic effective diffusivity calculated using in-plane percolation model, and (iii) anisotropic diffusivity calculated by percolation model. The anisotropic model considers variation of diffusivity in two directions only—in-plane and through-plane.

8.2.1. Mass diffusivity effects for low porosity PTL

We first present the simulation results for the case of PTL with a low porosity of 0.40, which is likely an unrealistic value but one that has been used commonly in PEMFC modeling literature. Fig. 7 presents simulation results for three different effective diffusivity models. Fig. 7(a and b) depicts the distribution of current at the membrane catalyst interface for two different load conditions, A and B indicated on cathode polarization curve, Fig. 7(c).

If we compare the two isotropic models, it can be observed that at both load conditions, the predicted current is everywhere lower in the case of the percolation model because of the lower effective mass diffusivity. This effect is more pronounced under the land area. The maximum decrease is on the order of 8% at

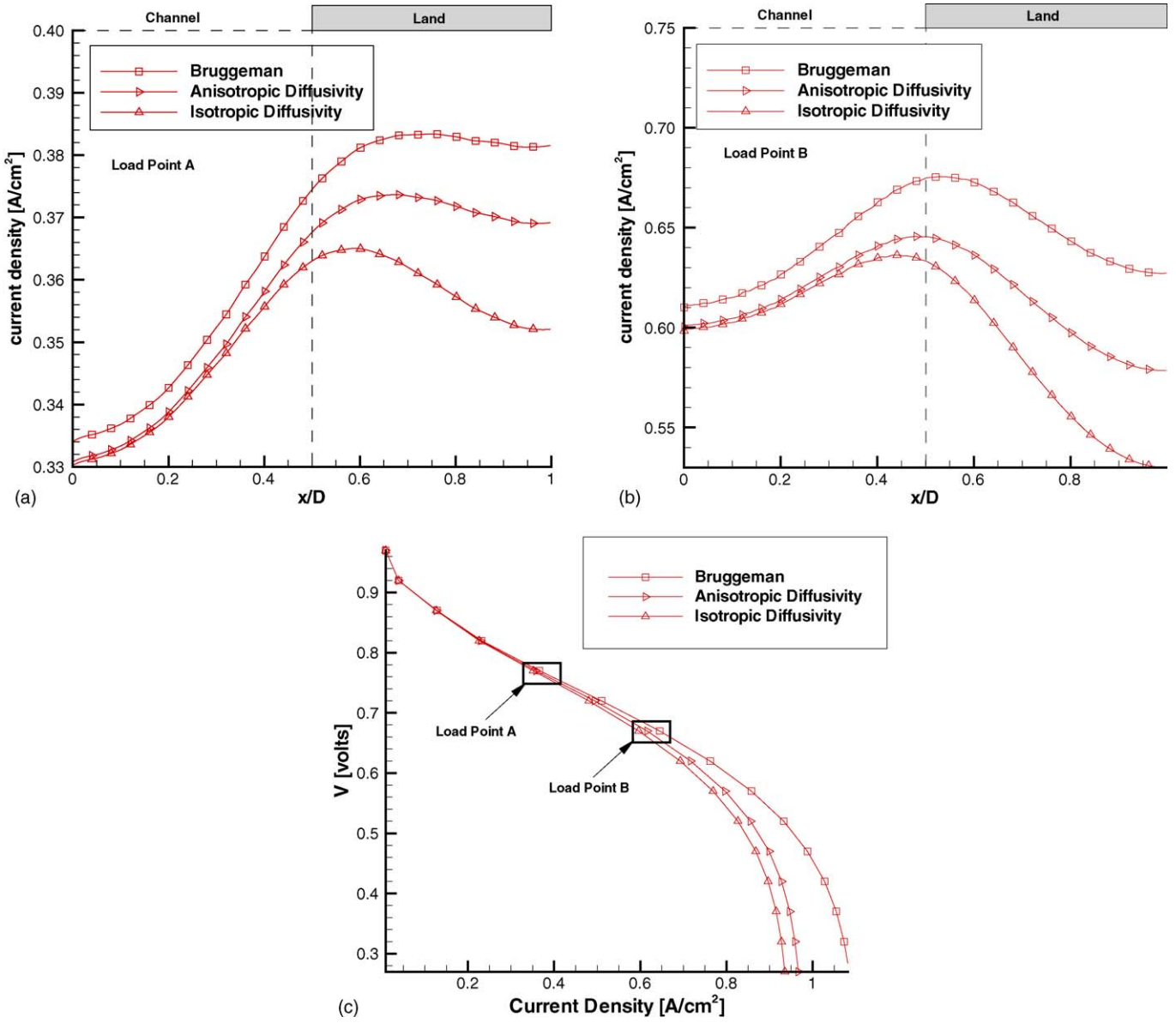

Fig. 7. Effect of diffusivity models on predicted (a–b) current density distributions and (c) polarization curves for PTL porosity of 0.4

the lower load condition and 16% at the higher load condition. It is also evident from the polarization curve, Fig. 7(c) that the onset of mass transfer limitations occurs at significantly lower currents with decreasing effective diffusivity. It is of note that the model employed to investigate these effects is a single phase model such that there is no liquid water present in any of the simulations. The sharp voltage drop off at higher currents can be attributed to a mass transfer resistance through the Nafion film which is assumed to surround each catalyst agglomerate [13]. The thickness of the Nafion film has been held constant for all cases considered herein.

Next, we consider the effect of anisotropic mass diffusivity, with both the in-plane and through-plane diffusivities determined from the percolation theory (Eq. (4). If we compare the isotropic percolation and anisotropic percolation models, it can be observed from Fig. 7(a and b) that there is a significant increase in the predicted current under the land, while the current under the channel remains virtually unchanged. This is due to the fact that the anisotropic model results in a relative increase in the through plane conductivity. Also evident is a slight increase in the maximum current predicted, consistent with the above arguments. An important point to be emphasized is that the PEMFC performance predicted using Bruggeman model is significantly higher than than anisotropic model.

8.2.2. *Mass diffusivity effects for high porosity PTL*

In this section we examine to what extent do the predictions from the three diffusivity models vary for an input PTL porosity of 0.6, a value more representative of a PTL in an operating PEMFC. Fig. 8(a and b) present the current density distribution for two different load conditions, B and C, indicated on cathode polarization curve, Fig. 8(c).

In comparison to results presented in preceding section (Fig. 7), several points may be noted. For PTL porosity of 0.6, each of the three models exhibit a limiting current density that is at least 20% higher than that for PTL porosity of 0.4 Examining

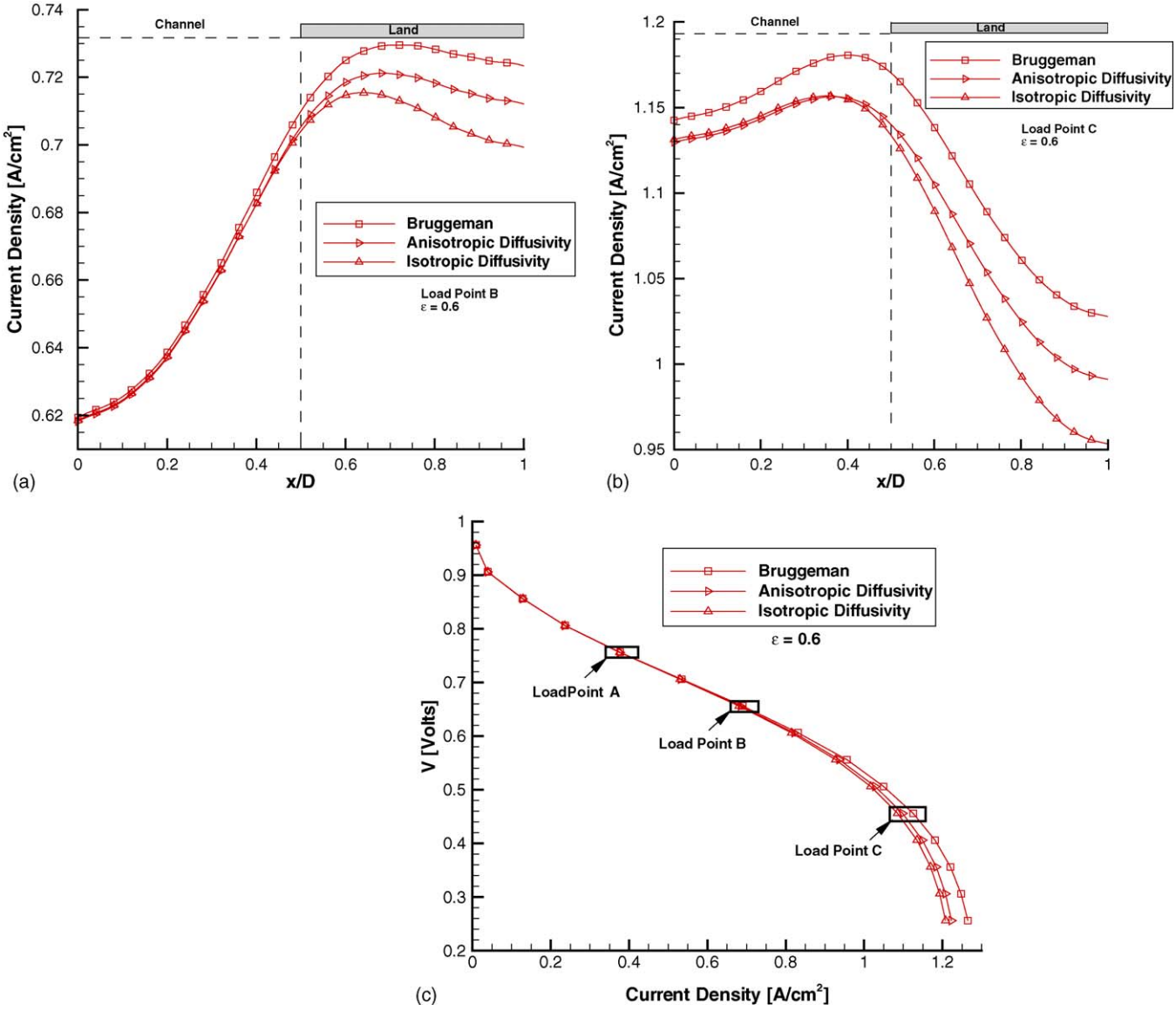

Fig. 8. Effect of diffusivity models on predicted (a–b) current density distributions and (c) polarization curves for PTL porosity of 0.6.

Figs. 7(c) and 8(c), it can be observed that differences in predictions from the three models begin to appear at Cathode potential of less than 0.8 V and less than 0.6 V for PTL porosities of 0.4 and 0.6, respectively. Comparing the current density distributions in Figs. 7(b) and 8(a) which correspond to load Point B, it can be concluded that upon increasing the PTL porosity from 0.4 to 0.6, the facility of oxygen transport vis-a-vis electron transport is enhanced. This effect is manifested in a higher current density generated being under the land than that under channel for PTL porosity of 0.6 For the case of PTL porosity of 0.6, the effect of mass transfer limitations become prominent at higher overpotential or lower cathode potential as observed in higher current densities under the land area in Fig. 8(b). An underlying point to be noted that the commonly employed Bruggeman relation predicts a higher current density compared to that by other models, although the differences are within 5–6%.

From the results presented in Sections 8.2.1 and 8.2.2, it is clear that predicted fuel cell performance is sensitive to the absolute value of the effective diffusivity used in the porous media. This value is currently not well represented by the Bruggeman relation originally developed for isotropic porous media composed of dense packings of solid spheres. It would be a significant advantage to fuel cell modelling if the determination of the effective diffusivity was a standard test in the characterization of fuel cell PTLs.

The local reaction rate is coupled to the local electronic potential, ionic potential, concentration and temperature through the Butler–Volmer equation. So far we have explored only the effect of concentration changes resulting from different effective diffusivities. We will now investigate the effect of electronic conductivity.

8.3. Isotropic and anisotropic electronic conductivity

As discussed earlier, it is expected that the electronic conductivity of fibrous PTL materials will be anisotropic although most

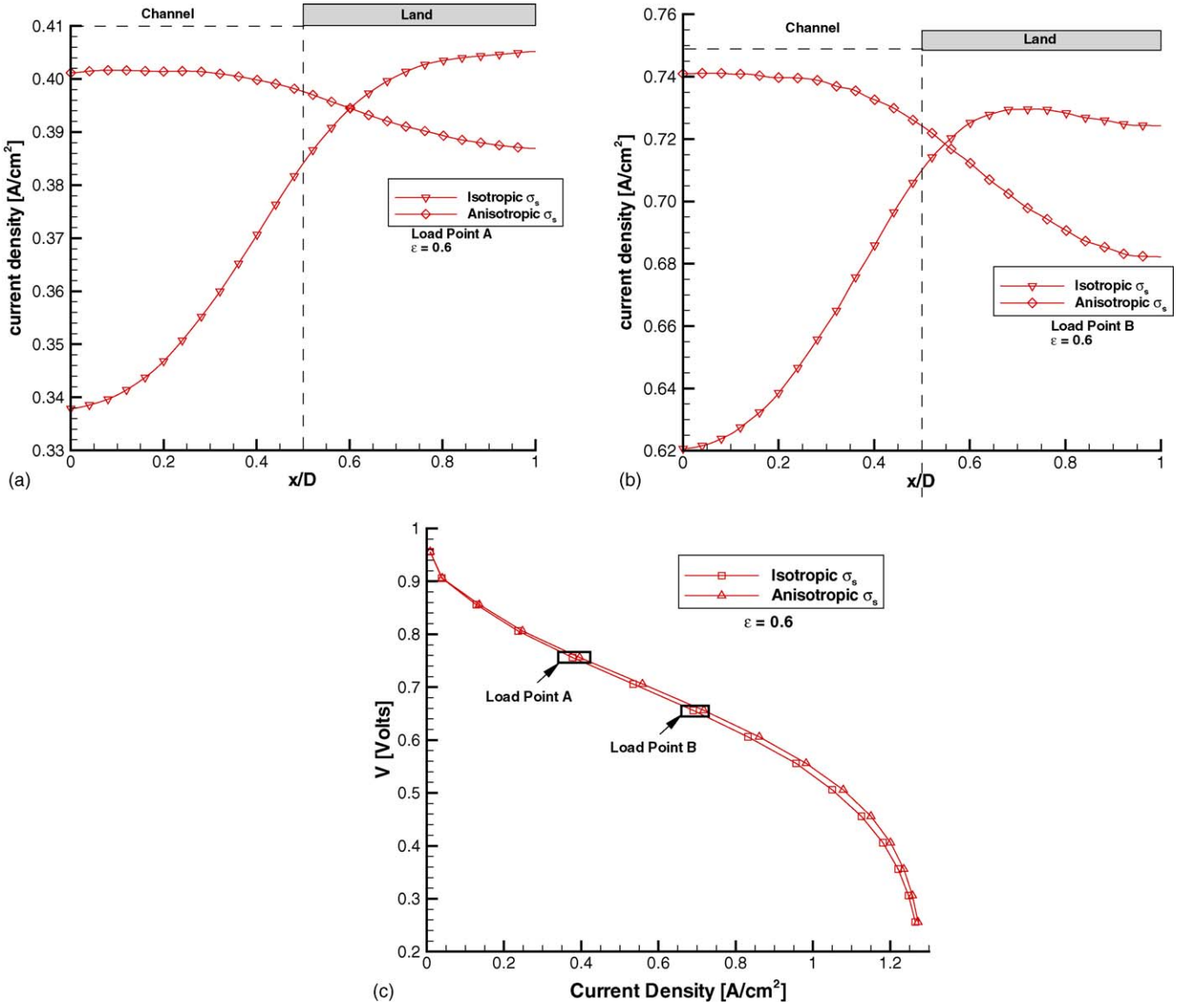

Fig. 9. Effect of anisotropic electronic conductivity on predicted (a–b) current density distribution and (c) polarization curves.

models assume isotropy. In order to quantify the effect of this assumptions two cases are compared: one assuming isotropic electronic conductivity, and the other with an in-plane conductivity one order of magnitude higher than the through-plane value. In order to isolate the effect of changes in electronic conductivity, the mass diffusivity is isotropic and described by the Bruggeman relation for the two cases.

Fig. 9(a and b) presents the current density distribution at the catalyst layer–PTL interface for two different load points A and B indicated on the polarization curve in Fig. 9(c). The same two load points for the cases of isotropic electronic conductivity and anisotropic electronic conductivity was maintained. In the case of isotropic electronic conductivity, for load point A the reaction is limited by the relatively low value of the conductivity ($100\,S\,m^{-1}$) such that the current is higher under the land area, with the maximum occurring under the land area. For load point A, as the current density is increased the location of maximum current is increased to region near the channel–land interface. For the case of anisotropic conductivity, because the in-plane electronic conductivity is 10-folds through-plane conductivity, the resistance to electron transport from land area to under the channel area is significantly reduced, and the maximum shifts to the channel centreline where the oxygen concentrations are highest.

This is an extremely interesting case, because the predicted polarization curves are almost identical, and yet the local current distribution is completely different. Unfortunately, the current method for validation of PEMFC models are based on comparing model predictions to experimental data for a single polarization curve. This remarkable coincidence illustrates the danger of attempting to validate fuel cell models using a single polarization curve. Clearly, the choice of physics modeled and the setting of the parameters in those models has a large impact on the detailed results. These differences, while significant for the design and optimization of fuel cells are completely obscured upon integration to the polarization curve.

Fuel cell models require many transport and reaction parameters, many of which are currently not well characterized. It is crucial to recognize the physical basis for these parameters, and to account for the microstructure of the electrodes used in the fuel cell being modeled. In some cases certain physics are neglected in a model and the one or more remaining parameters are tuned to match a single polarization curve. This will clearly detract from the predictive capability of the derived model. It is our opinion that model validation must involve, at a minimum, agreement with multiple polarization curves taken under different operating conditions or with different fuel cell components relevant to the study in question.

9. Conclusions

In this paper, the approach taken in the literature to describe effective transport coefficients of porous PEMFC electrodes was reviewed. It was concluded that a majority of the existing PEMFC models volume-average the effect of porous media using a function that assumes the electrode to be isotropic. This is despite the fact that the inherently anisotropic microstructure of the porous carbon-fibre electrode results in a distinctly different effective mass diffusivity, electronic conductivity, thermal conductivity, and hydraulic permeability in the through-plane and the in-plane directions.

Using a 2-D PEMFC cathode model, it was shown that treating the electrodes as an isotropic porous media yields significantly different current density predictions than anisotropic treatments. Most importantly, it was demonstrated that for certain sets of parameters, both isotropic and anisotropic models yield virtually identical polarization curves, however, the current density distributions are completely different. This result highlights the danger of validating detailed PEMFC models with a single set of data, namely, the polarization curve. More importantly, it clearly identifies the need for appropriately characterizing the effective transport coefficients of the porous such that correct representation of the microstructural effects and physics of the processes are accounted for. At a minimum, correct porosity of the PTL must be determined under realistic conditions. The spatial variation of porosity must be also of accounted for in the PEM models.

Acknowledgments

The authors would like to acknowledge Natural Sciences and Engineering Council of Canada (NSERC) and Queen's University for financial assistance. We are also thankful to the vibrant fuel cell community at the Queen's-RMC Fuel Cell Research Centre and, in particular, the members of the student fuel cell network for many stimulating discussions.

References

[1] K.Z. Yao, K. Karan, K.B. McAuley, P. Oosthuizen, B. Peppley, T. Xie, A review of mathematical models for hydrogen and direct methanol polymer electrolyte membrane fuel cells, Fuel Cells Fundam. Syst. 4 (2004) 3–29.
[2] M. Mathias, J. Roth, J. Fleming, W. Lenhert, Diffusion media materials and characterization, in: Handbook of Fuel Cells—Fundamentals, Technology and Applications, vol. 3, John Wiley and Sons, 2003.
[3] J.G. Pharoah, On the permeability of gas diffusion media used in PEM fuel cells, J. Power Sources 144 (2005) 72–82.
[4] D.A.G. Bruggeman, Calculation of the various physical constants of heterogeneous substances. i: Dielectric constants and conductivities of mixtures of isotropic substances, Ann. Physik. 25 (1935) 636–664.
[5] R.E. De La Rue, C.W. Tobias, On the conducticity of dispersions, J. Electrochem. Soc. 106 (9) (1959) 827–833.
[6] J.H. Nam, M. Kaviany, Effective diffusivity and water-saturation distribution in single- and two-layer PEMFC diffusion medium, Int. J. Heat Mass Trans. 46 (2003) 4595–4611.
[7] M.M. Tomadakis, S.V. Sotirchos, Effective knudson diffusivitiews in structures of randomy overlapping fibers, AIChE J. 37 (1) (1991) 74–86.
[8] M.M. Tomadakis, S.V. Sotirchos, Ordinary and transition regime diffusion in random fiber structures, AIChE J. 39 (3) (1993) 397–412.
[9] T. Berning, N. Djilali, A 3D, multiphase, multicomponent model of the cathode and anode of a pem fuel cell, J. Electrochem. Soc. 150 (12) (2003) A1589–A1598.
[10] P.J.S. Vie, S. Kjelstrup, Thermal conductivities from temperature profiles in the polymer electrolyte fuel cell, Electrochim. Acta 49 (2004) 1069–1077.
[11] D.J. Hamilton. A numerical method to determine effective transport coeffcients in porous media with application to pem fuel cells, M.Sc. Thesis, Queen's University at Kingston, 2005.

[12] B.R. Sivertson, N. Djilali, Cfd-based modelling of proton exchange membrane fuel cells, J. Power Sources 141 (2005) 65–78.
[13] W. Sun, B.A. Peppley, K. Karan, An improved two-dimensional agglomerate cathode model to study the influence of catalyst layer structural parameters, Electrochim. Acta 50 (1) (2005) 3359–3374.
[14] H. Meng, C.Y. Wang, Electron transport in PEFCs, J. Electrochem. Soc. 151 (3) (2004) A358–A367.
[15] W. Sun, B.A. Peppley, K. Karan, Modeling the influence of gdl and flow-field plate parameters on the reaction distribution in the pemfc cathode catalyst layer, J. Power Sources 144 (2005) 42–53.
[16] F. Barbir, H. Gorgun, X. Wang, Relationship between pressure drop and cell resistance as a diagnostic tool for PEM fuel cells, J. Power Sources 141 (1) (2005) 96–101.
[17] B. Tysoe, Numerical and experimental determination of in-plane permeability of the porous transport layer in proton exchange membrane fuel cells, M.Sc. Thesis, Queen's University at Kingston, in preparation.
[18] F. Yang, V. Mishra, R. Pitchumani, Measurement and prediction of electrical contact resistance between gas diffusion layers and bipolar plate for applications to pem fuel cells, J. Fuel Cell Sci. Technol. 1 (2004) 2–9.
[19] J.T. Gostick, M.W. Fowler, M.A. Ioannidis, M.D. Pritzker, Y.M. Volfkovich, A. Sakars, Capillary pressure and hydrophilic porosity in gas diffusion layers for polymer electrolyte fuel cells, J. Power Sources 156 (2) (2006) 375–387.
[20] T.E. Springer, T.A. Zawodzinski, S. Gottesfeld, Polymer electrolyte fuel cell model, J. Electrochem. Soc. 138 (8) (1991) 2334–2341.